PROC: OF JSCE
No. 311, July 1981

FINITE ELEMENT APPROXIMATIONS OF SMOOTH CONTACT-IMPACT PROBLEMS

By Katsumi KAMEMURA and June K. LEE***

ABSTRACT

This study is concerned with finite element models and solution algorithms for a class of contact-impact problems which are formulated within the frame-work of the modern theory of variational inequalities. Discussions are limited to smooth contact-impact of a linearly elastic body to a rigid support.

A brief review on two distinct variational formulations and associated algorithms is first given and then a new algorithm based on reciprocal formulation is proposed. According to presented numerical experiments, the new algorithm converges rather rapidly and is easy to use. Numerous examples including classical contact, rigid punch, and transient analyses of impact problems are presented and discussed. Possible extensions of the current study are also discussed.

1. INTRODUCTION

The classical contact-impact problems involving simple geometrical shapes are well documented in the book by Goldsmith[1]. Although the contributions made by the finite element method in many areas of analysis are paramount, very few capabilities are available to handle contact-impact effects largely due to difficulties in handling contact conditions. A fast and general algorithm based on a sound formulation capable of treating contact impact condition is in need.

This study is concerned with finite element models and solution algorithms for a class of smooth elastic contact-impact problems based on the variational inequality formulation. A rigorous mathematical discription of contact condition in connection with variational inequalities was given by Signorini[2] and Fichera[3]. Lions and Stampacchia[4] extended the theory of variational inequalities. Use of inequality constraints and variational formulation are well documented in the book by Duvaut and Lions[5]. Having inequality constraints on displacement and stress on contact surface, variational inequality formulations seem very natural and attractive to finite element models.

Engineering type of approach ranges from typical trial and error method (see, for example,[6]) to quite elaborate scheme proposed by Hughes, *et al.*[7]. Reported numerical examples look impressive but variational formulations are mostly of ad-hoc characters. A bit more mathematically oriented work involves, most of the time, a variational formulation suitable to use a particular type of optimization technique.

Kalker and Van Randen[8] solved non-Hertzian half space problems by applying minimum energy principle and a quadratic programing method. Similar approach was also reported by Conry and Seireg[9]. Kalker summarized variational principles used up to 1976 later in 10).

Woodword and Paul[11] developed a numerical technique of solving singular integral equations, which can be applied to Hertzian and non-Hertzian problems. However, the geometry of boundary plays a critical role in the formulation of integral equation and study was limited to spherical shapes.

Panagiotopoulos[12] discussed potential and complementary energy principles suitable for an optimization technique to solve elastic contact to inelastic foundation. It was noted in 12) that the convergence cannot be guaranteed when a trial and error approach is used.

Fremond[13] treated the potential energy principle with inequality constraint using the Lagrange multiplier, which is briefly reviewed in section 2.(2).

Kikuchi[14] introduced reciprocal formulation by using Green's function. Beauty of this method is that inequalities appear only on the possible contact boundary in terms of the contact

* Member of JSCE, Research Engineer, Taisei Corporation.
** Assistant Proffessor, Department of Engineering Mechanics, The Ohio State University, U.S.A.

pressure P and the system of inequalities become smaller compared to one given by Fremond.

This study starts from the formulation given by Kikuchi. A new solution algorithm for the resulting finite element reciprocal inequalities is proposed in section 2.(4) and evaluated via numerical experiments in section 2.(5).

In chapter 3, the basic concepts of treating contact condition is extended to solve impact problems. Release condition is found to be as important as the contact condition in this case. When a time stepping method is used, one must check contact and release condition for each time step. For this reason, rapidly converging algorithm and relatively small number of inequalities are desirable. The proposed algorithm together with the reciprocal formulation seems to fit here very well. Numerical examples include impact of an elastic bar and sphere.

2. SMOOTH CONTACT OF ELASTO STATICS

(1) Contact Condition

Consider a regular and bounded elastic body Ω making a smooth contact against a rigid surface as shown in **Fig. 1**. The boundary Γ will be assumed to be smooth and consists of displacement boundary Γ_D, traction boundary Γ_T, and possible contact surface of the undeformed body Γ_C, so that

$$\Gamma=\Gamma_D\cup\Gamma_T\cup\Gamma_C \quad \cdots\cdots(2.1)$$

$$\Gamma_D\cap\Gamma_T=\phi,\quad \Gamma_T\cap\Gamma_C=\phi,\quad \Gamma_C\cap\Gamma_D=\phi \quad \cdots\cdots(2.2)$$

and

$$u_i=U_i \quad \text{on } \Gamma_D \quad \cdots\cdots(2.3)$$

$$\sigma_{ij}n_j=T_i \quad \text{on } \Gamma_T \quad \cdots\cdots(2.4)$$

where

ϕ : null set
u_i : displacement vector
$\boldsymbol{U}=\{U_i\}$: prescribed displacement vector
σ_{ij} : component of stress tensor
n_j : component of outer unit normal vector on Γ
$\boldsymbol{T}=\{T_i\}$: prescribed surface traction

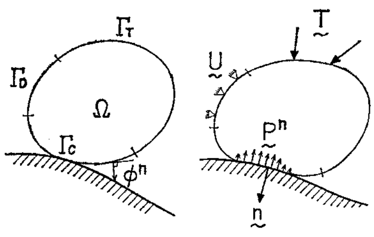

Fig. 1 A contact problem under consideration.

Henceforth the usual summation convention is enployed over the repeated indicies.

On the possible contact boundary Γ_C, we introduce $\phi^n(\boldsymbol{x})$, the normal distance between the rigid surface and Γ_C, and let σ^n and u^n be the normal stress and displacement on Γ_C. Then the displacement and the normal stress must satisfy

$$u^n-\phi^n\leq 0 \quad \cdots\cdots(2.5)$$

and

$$\sigma^n=0 \quad \text{if } u^n-\phi^n<0 \quad \cdots\cdots(2.6)$$

$$\sigma^n=P^n\leq 0 \quad \text{if } u^n-\phi^n=0 \quad \cdots\cdots(2.7)$$

where P^n is unknown normal component of contact stress. For a smooth contact,

$$\sigma^T=P^T=0 \quad \cdots\cdots(2.8)$$

where σ^T is the tangential stress on Γ_C and P^T is the tangential component of surface traction due to the friction. Contact conditions (2.5)~(2.7), can be written in a more convenient form:

$$\left.\begin{array}{ll}\sigma^n(u^n-\phi^n)=0, & \sigma^n\leq 0,\\ u^n-\phi^n\leq 0 & \text{on } \Gamma_C\end{array}\right\} \quad \cdots\cdots(2.9)$$

The smooth contact problem of elasto statics is to find the displacement field $\boldsymbol{u}$ and stress σ, which satisfy the inequalities (2.9) and the following basic equations of elastic continuum:

equilibrium equation:

$$\sigma_{ij,j}+f_i=0 \quad \cdots\cdots(2.10)$$

constitutive equation:

$$\sigma_{ij}=E_{ijkl}\epsilon_{kl} \quad \cdots\cdots(2.11)$$

strain displacement relation:

$$\epsilon_{ij}=\frac{1}{2}(u_{i,j}+u_{j,i}) \quad \cdots\cdots(2.12)$$

where

f_i: component of body force
E_{ijkl}: elasticity tensor
ϵ_{ij}: component of strain tensor

Kalker and Van Randen[8] presented two variational principles for this problem. They are:

(i) minimize potential energy U subjected to the constraint

$$u^n-\phi^n\leq 0$$

(ii) minimize "contact enthalpy" H subjected to the constraint

$$\sigma^n\leq 0$$

where H is defined as

$$H=\int_{\Gamma_C}\sigma^n(u^n-\phi^n)\,d\Gamma-U \quad \cdots\cdots(2.13)$$

As shown in the following sections, Primal Method by Fremond belongs to (i) and the reciprocal (or Dual) method studied by Kikuchi can be derived from (ii). A proper optimization technique can be used to minimize the functional subjected to inequality constraints.

When the usual finite element method (c.f. 16) or 17)) is applied, we have, using the index notations,

$$K_{\alpha i\beta k}\cdot u_{\beta k}=f_{\alpha i} \quad \cdots\cdots(2.14)$$

where

$$K_{\alpha i\beta k}=\int_{\Omega} N_{\alpha,j}E_{ijkl}N_{\beta,l}\,d\Omega \quad \cdots\cdots(2.15)$$

$$f_{\alpha i}=\int_{\Omega} N_\alpha f_i\,d\Omega-\int_{\Gamma_T} N_\alpha T_i\,d\Gamma \quad \cdots\cdots(2.16)$$

In these equations, lower case Greek letters (α, β, ...) and lower case Latin letters (i, j, k, ...) represent the node number and the direction of reference frame, respectively. For example, $u_{\beta k}$ is the x_k direction displacement at β-th node. N_α is a proper interpolation function associated with α-th node so that

$$u_i(\boldsymbol{x})\approx N_\alpha(\boldsymbol{x})u_{\alpha i} \quad \cdots\cdots(2.17)$$

For a notational convenience the same symbols are used for both exact and approximate quantities.

The discrete boundary and contact conditions can be written as

$$u_{\beta k}=U_{\beta k} \quad \text{on } \Gamma_D \quad \cdots\cdots(2.18)$$

$$\left.\begin{array}{ll} P^n_\alpha(u^n_\alpha-\phi^n_\alpha)=0\,, & P^n_\alpha\leq 0\,, \\ u^n_\alpha-\phi^n_\alpha\leq 0 & \text{on } \Gamma_C \end{array}\right\} \quad \cdots\cdots(2.19)$$

where P^n_α is unknwon contact force at node α.

(2) Primal Method

Following Fremond[13] or according to (i) of section 2.(1), the discretized contact condition in terms of the primal variable $\boldsymbol{u}$ can be written as

$$M^n_{\alpha\beta i}u_{\beta i}-\phi^n_\alpha\leq 0 \quad \cdots\cdots(2.20)$$

where $M^n_{\alpha\beta i}$ is a transformation matrix such that

$$M^n_{\alpha\beta i}u_{\beta i}=u^n_\alpha \quad \text{on } \Gamma_C \quad \cdots\cdots(2.21)$$

Then the discretized variational problem is

$$\inf\left\{\frac{1}{2}u_{\alpha i}K_{\alpha i\beta k}u_{\beta k}-f_{\alpha i}u_{\alpha i}\,|\,M^n_{\alpha\beta i}u_{\beta i}-\phi^n_\alpha\leq 0\right\} \quad \cdots\cdots(2.22)$$

Since the matrix $M^n_{\alpha\beta i}$ is not positive definite in general, difficulties arise in the application of minimization method. In order to avoid these difficulties, the Lagrange multiplier μ_α is introduced and the condition (2.20) is re-written into an equivalent form:

$$\sup_{\mu_\alpha\geq 0}\{\mu_\alpha(M^n_{\alpha\beta i}u_{\beta i}-\phi^n_\alpha)\}=0 \quad \cdots\cdots(2.23)$$

Then the problem (2.22) is equivalent to

$$\left.\begin{array}{l} \inf\limits_{u}\sup\limits_{\mu_\alpha\geq 0}\left\{\frac{1}{2}u_{\alpha i}K_{\alpha i\beta k}u_{\beta k}-f_{\alpha i}u_{\alpha i}+\mu_\alpha(M^n_{\alpha\beta i}u_{\beta i}-\phi^n_\alpha)\right\} \\ \text{or} \\ \sup\limits_{\mu_\alpha\geq 0}\inf\limits_{u}\left\{\frac{1}{2}u_{\alpha i}K_{\alpha i\beta k}u_{\beta k}-f_{\alpha i}u_{\alpha i}+\mu_\alpha(M^n_{\alpha\beta i}u_{\beta i}-\phi^n_\alpha)\right\} \end{array}\right\} \quad \cdots\cdots(2.24)$$

This can be solved by Uzawa's iterative method (UIM) (c.f. 15)), consisting of the following steps:

Step 1: choose any $\mu^{(0)}_\alpha\geq 0$

Step 2: find $u^{(n)}_{\beta k}$ by solving

$$\inf\left\{\frac{1}{2}u_{\alpha i}K_{\alpha i\beta k}u_{\beta k}-f_{\alpha i}u_{\alpha i}+\mu^{(n)}_\alpha(M^n_{\alpha\beta i}u_{\beta i}-\phi^n_\alpha)\right\}$$

$$\rightarrow\quad K_{\alpha i\beta k}u^{(n)}_{\beta k}=f_{\alpha i}-\mu^{(n)}_\beta M^n_{\beta\alpha i} \quad \cdots\cdots(2.25)$$

Step 3:

$$\text{set } \mu^{(n+1)}_\alpha=\sup\{0,\ \mu^{(n)}_\alpha+\theta(M^n_{\alpha\beta i}u^{(n)}_{\beta i}-\phi^n_\alpha)\} \quad \cdots\cdots(2.26)$$

Step 2 and 3 are repeated until $u^{(n)}_{\beta k}$ converges within a certain tolerance. For the convergency of the algorithm, the positive parameter θ must be in the region $(o,\ 2A/B^2)$, where A and B are the smallest and largest eigen values of a matrix which depends on $M^n_{\alpha\beta i}$ and $K_{\alpha i\beta k}$.

As shown in (2.25), in this algorithm the entire system of equations must be solved for each iteration. Moreover, convergence depends heavily on the choice of the iteration parameter θ in (2.26). When iteration converges, the multiplier μ_α turns out to be the nodal contact force. For a practical application of this method, a realistically computable bound on the parameter θ need to be made.

(3) Reciprocal Formulation and Pointwise Relaxation Method

For a linear elastic problem, by making use of the method of superposition and the Green's function, one can write

$$\boldsymbol{u}=\hat{\boldsymbol{u}}+G(P) \quad \cdots\cdots(2.27)$$

where $\hat{\boldsymbol{u}}=G(\boldsymbol{f},\ \boldsymbol{T})$ is the displacement due to the applied body force and prescribed surface traction without considering contact condition, G is the Green's operator, and $G(P)$ is the additional displacement due to the contact force P. Then the contact condition takes the form,

$$\left.\begin{array}{ll} P\{G(P)^n-\hat{\phi}^n\}=0 & \\ P\leq 0\,,\quad G(P)^n-\hat{\phi}^n\leq 0 & \text{on } \Gamma_C \end{array}\right\} \quad \cdots\cdots(2.28)$$

where

$$\hat{\phi}^n=\phi^n-\hat{u}^n \quad \cdots\cdots(2.29)$$

with $\hat{\phi}^n$ being the original normal distance between two bodies (c.f. Fig. 1). From condition (2.28), the following variational problem can be derived[14]; namely find $P\leq 0$ such that

$$\left.\begin{array}{l}\int_{\Gamma_C}\{G(P)^n-\hat{\phi}^n\}(Q-P)\,d\Gamma\geq 0\\ \quad\forall Q\leq 0\end{array}\right\}\quad\cdots\cdots(2.30)$$

It can be shown that (2.30) is equivalent to (2.28) by taking $Q=0$ and $Q=2P$.

Introducing a finite element approximation, the Green's operator can be approximated by the inverse of the stiffness matrix. Then the discrete form corresponding to the problem (2.30) is to find.

$$\left.\begin{array}{l}P_\alpha^n\in K:\ \int_{\Gamma_C}(C_{\alpha\beta}P_\beta^n-\hat{\phi}_\alpha^n)(q_\alpha^n-P_\alpha^n)\,d\Gamma\geq 0\\ \qquad\forall q_\alpha^n\in K\end{array}\right\}\quad\cdots\cdots(2.31)$$

$$K=\{q_\alpha^n\in\boldsymbol{R}^m:\ q_\alpha^n\leq 0\}\quad\cdots\cdots(2.32)$$

where m is the total degree of freedom on Γ_C and $C_{\alpha\beta}$ is $m\times m$ matrix defined by

$$C_{\alpha\beta}=n_i^{(\alpha)}K_{\alpha i\beta k}^{-1}n_k^{(\beta)}\quad\cdots\cdots(2.33)$$

where $n_i^{(\alpha)}$ and $n_k^{(\beta)}$ are the component of the outer unit normal vector at α-th and β-th nodes, respectively. It should be noted that the variational inequality (2.31) is defined only on the possible contact surface Γ_C. The solution P of (2.31) satisfies the following discrete contact condition.

$$\left.\begin{array}{l}P_\alpha^n(C_{\alpha\beta}P_\beta^n-\hat{\phi}_\alpha^n)=0,\quad C_{\alpha\beta}P_\beta^n-\hat{\phi}_\alpha^n\leq 0,\\ P_\alpha^n\leq 0\end{array}\right\}\quad\cdots\cdots(2.34)$$

Kikuchi[14] proposed to use the projectional pointwise relaxation method (PPRM) consisting of following steps;

Step 1: solve $K_{\alpha i\beta k}\hat{u}_{\beta k}=f_{\alpha i}$

Step 2: compute $\hat{\phi}_\alpha^n=\phi_\alpha^n-\hat{u}_\alpha^n$ and form $C_{\alpha\beta}$ as in (2.33)

Step 3: put $P_\alpha^n(0)=0$

Step 4: calculate $P(t+1)$ by

$$P_\alpha^n\left(t+\frac{1}{2}\right)=(1-\omega)P_\alpha^n(t)-\omega\left\{\sum_{\beta=1}^{\alpha-1}C_{\alpha\beta}P_\beta^n(t+1)-\sum_{\beta=\alpha+1}^{m}C_{\alpha\beta}P_\beta^n(t)-\hat{\phi}_\alpha^n\right\}\Big/C_{\alpha\alpha}$$

$$P_\alpha^n(t+1)=\min\left\{P_\alpha^n\left(t+\frac{1}{2}\right),\ 0\right\}$$

Step 5: if $|P_\alpha^n(t+1)-P_\alpha^n(t)|\leq\epsilon$ go to Step 6
if $|P_\alpha^n(t+1)-P_\alpha^n(t)|>\epsilon$ go to Step 4

Step 6: calculate the additional displacement

$$u_{\beta k}=\hat{u}_{\beta k}+K_{\alpha i\beta k}^{-1}P_\alpha^n n_k^{(\alpha)}$$

This iteration algorithm will converge with the iteration factor ω: $0<\omega<2$, if the matrix $C_{\alpha\beta}$ is positive definite. Numerical experiments show relatively good convergence, requiring 20~30 iterations. For a detail, see 14) and 18) for various variational formulations and solution techniques.

(4) Elimination Method

A new and fast converging solution algorithm for the discrete contact condition (2.34) is proposed here. Referring to inequality (2.34), suppose that Γ_C is the true contact boundary, then we must have

$$\left.\begin{array}{ll}C_{\alpha\beta}P_\alpha^n-\hat{\phi}_\alpha^n=0 & \text{and}\\ P_\beta^n=C_{\alpha\beta}^{-1}\hat{\phi}_\alpha^n\leq 0 & \text{on }\Gamma_C\end{array}\right\}\quad\cdots\cdots(2.36)$$

This means, if $\hat{\phi}_\alpha^n$ is applied to the true contact boundary, the resultant P_α^n is true contact force. In the case that Γ_C is not the true contact boundary including the true one, applied $\hat{\phi}_\alpha^n$ yields some false contact forces, i.e. positive value of P_α^n on the false contact boundary. Thus we eliminate this part from the possible contact boundary and solve (2.36) for the eliminated boundary. This procedure is repeated until (2.36) is satisfied. The algorithm based on elimination process can be summarized in the following steps;

Step 1: solve $K_{\alpha i\beta k}\hat{u}_{\beta k}=f_{\alpha i}$

Step 2: compute $\hat{\phi}_\alpha^n=\phi_\alpha^n-\hat{u}_\alpha^n$ and form $C_{\alpha\beta}$

Step 3: solve $P_\beta^n=C_{\alpha\beta}^{-1}\hat{\phi}_\alpha^n$

Step 4: if $P_\beta^n\leq 0$ for each β go to Step 5
if $P_\beta^n>0$ for some β eliminate corresponding rows and columns of $C_{\alpha\beta}$ and go to Step 3

Step 5: calculate the correct displacement by

$$u_{\beta k}=\hat{u}_{\beta k}+K_{\alpha i\beta k}^{-1}P_\alpha^n n_k^{(n)}$$

As long as the possible contact boundary Γ_C contains the true contact boundary, this alogorithm is very effective and converges rapidly. For an excessively large system with a large contact surface, this algorithm may be too expensive. Further developments are needed.

(5) Numerical Examples

In order to compare discussed solution algorithms, simple examples including a Hertzian contact problem and rigid punch problems are solved. Computations are done on AMDAHL 470 using double precision.

Finite element mesh, boundary conditions and material properties for a Hertzian contact problem are shown in **Fig. 2**. **Fig. 3** shows the distribution of contact pressure calculated from the difinition of the nodal contact force. The number of iteration and the c.p.u. time of three solution algroithms are compared (when F: contact force $F=240$) in **Table 1** which shows the proposed elimination method requires the

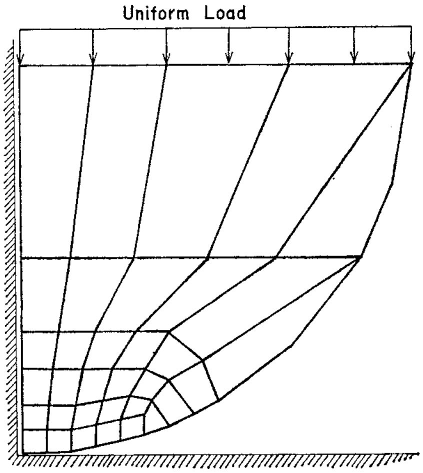

Fig. 2 Finite element mesh for Hertz's contact problem.

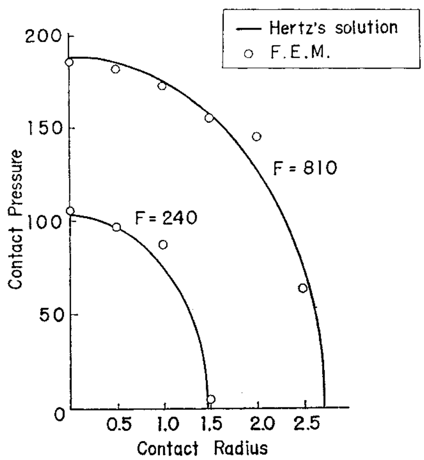

Fig. 3 Contact pressure distribution.

Table 1 Comparison of convergency (Contact problem).

	Iteration	c.p.u. (sec)
inverse of 92×92 matrix		3.23
calculation of contact force		
i) P-UIM (c.f. section 2.(2) and 13))		
$\theta=5$	100 (not converged)	2.80
$\theta=10$	100 (not converged)	2.86
$\theta=50$	78	2.18
$\theta=100$	100 (oscillation)	2.81
$\theta=300$	100 (oscillation)	2.83
ii) R-PPRM (c.f. section 2.(3) and 14))		
$\omega=0.5$	35	0.09
$\omega=0.75$	26	0.07
$\omega=1.0$	22	0.07
$\omega=1.2$	25	0.07
$\omega=1.75$	92	0.16
iii) Elimination method (c.f. section 2.(4))	4	0.02

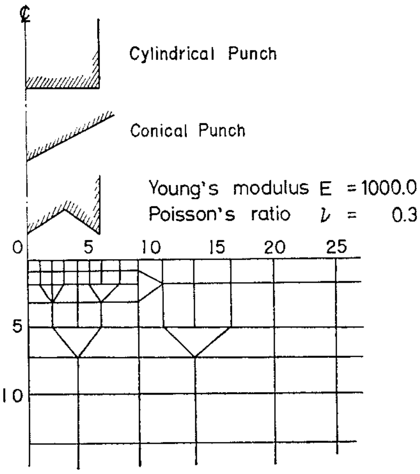

Fig. 4 Finite element mesh for rigid punch problem.

least computational effort. As expected, when converged, all three method give the same result. All units are in non-dimension.

Rigid punch problem can be solved by the same formulation as shown in 14) if the plane of indentation is known. The contact condition takes the form

$$\left.\begin{aligned} &u^n-a^n-\phi^n\leq 0\\ &\sigma^n=0 \quad \text{if } u^n<a^n-\phi^n\\ &\sigma^n\leq 0 \quad \text{if } u^n=a^n-\phi^n \end{aligned}\right\}\quad\cdots\cdots\cdots\cdots(2.40)$$

where a^n is the given normal displacement, i.e. the depth of indentation. The same algorithms discussed before can be applied to solve rigid punch problems.

Selected shapes of indentors along with a portion of mesh consisting of 78 four-node elements and 98 nodal points are shown in **Fig. 4**.

Fig. 5 shows the surface displacement near the punch. For the cases of cylindrical and conical punch, numerical results are compared with analytical solutions (see 19) and 20)), which show very good agreements. The punching force for conical and cylindrical punch problems is shown in **Table 2**. Numerical solutions are larger than analytical solutions for every case. This is because of the coarse mesh, the element singularity at the axis of symmetry and the finite reiong

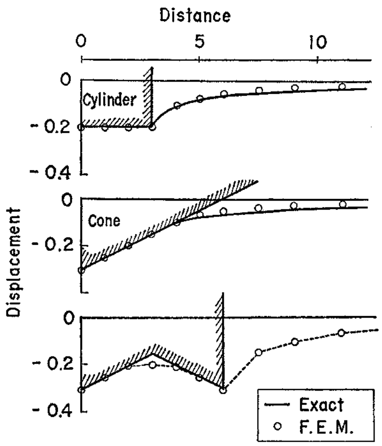

Fig. 5 Surface displacement for rigid punch problem.

Table 2 Punching force.

Max Disp	FEM	EXACT	Error (%)
(1) Conical punch (semivertical angle $\alpha=\pi/4$)			
1.0	758.9	699.6	8.5
2.0	3 303.7	2 798.3	18.1
3.0	7 098.2	6 296.3	12.7
(2) Conical punch (semivertical angle $\alpha=1.107$)			
1.0	1 651.8	1 399.2	18.1
2.0	6 284.3	5 596.7	12.3
3.0	1 5020.7	12 592.5	19.3
(3) Cylindrical punch			
0.2	1 636.3	1 318.7	24.1

Table 3 Comparison of convergency (Rigid punch problem).

	Iteration	c.p.u. (sec)
inverse of 196×196 matrix		31.02
calculation of punching force		
i) P-UIM (c.f. section 2.(2) and 13))		
$\theta=50$	100 (not converged)	
$\theta=300$	100 (not converged)	
$\theta=1\,000$	100 (not converged)	
$\theta=2\,000$	100 (not converged)	
ii) R-PPRM (c.f. section 2.(3) and 14)) $\omega=1.5$	5	0.15
iii) Elimination method (c.f. section 2.(4))	3	0.01

which should be infinite.

The c.p.u. time of three solution algorithms are compared in **Table 3** for the conical punch problem.

According to the presented numerical results, it is evident that

(i) The primal method requires a far more number of iteration due to implicit range of iteration factor θ and more computing time than others.

(ii) The proposed elimination method with the reciprocal formulation is very effective and converges very rapidly, which makes it very attractive to apply to transient analysis.

3. TRANSIENT ANALYSIS OF SMOOTH IMPACT PROBLEMS

(1) Impact and Release Condition

A smooth impact problem of linear elastic materials can be derived simply by adding an inertia term and initial conditions to an elasto static problem discussed in Section 2. (1). Thus the problem is to find the displacement $\boldsymbol{u}(\boldsymbol{x}, t)$ satisfying

equilibrium equation:

$$\rho\ddot{u}_i=\sigma_{ij,j}+f_i \quad \cdots\cdots(3.1)$$

constitutive equation:

$$\sigma_{ij}=E_{ijkl}\epsilon_{kl} \quad \cdots\cdots(3.2)$$

strain displacement relation:

$$\epsilon_{ij}=\frac{1}{2}(u_{i,j}+u_{j,i}) \quad \cdots\cdots(3.3)$$

where ($\dot{}$) indicates the differentiation with respect to time, subjected to

initial conditions:

$$\left.\begin{array}{l}\boldsymbol{u}(\boldsymbol{x},0)=\boldsymbol{u}_0(\boldsymbol{x})\\ \dot{\boldsymbol{u}}(\boldsymbol{x},0)=\dot{\boldsymbol{u}}_0(\boldsymbol{x})\end{array}\right\} \quad \cdots\cdots(3.4)$$

boundary conditions:

$$u_i=U_i \quad \text{on } \Gamma_D\times(0,T) \quad \cdots\cdots(3.5)$$

$$\sigma_{ij}u_j=T_i \quad \text{on } \Gamma_T\times(0,T) \quad \cdots\cdots(3.6)$$

contact conditions:

$$\sigma^T=0 \quad \text{(no friction)}$$

$$\left.\begin{array}{ll}P^n(u^n-\phi^n)=0, & P^n\leq 0,\\ u^n-\phi^n\leq 0 & \text{on } \Gamma_C\times(0,T)\end{array}\right\} \quad \cdots\cdots(3.7)$$

The associated discrete problem can be stated as ; find u_i such that

$$M_{\alpha\beta}\ddot{u}_{\beta i}+K_{\alpha i\beta k}u_{\beta k}=f_{\alpha i} \quad \cdots\cdots(3.8)$$

subjected to

$$\left.\begin{array}{ll}P_\alpha^n(u_\alpha^n-\phi_\alpha^n)=0, & P_\alpha^n\leq 0,\\ u_\alpha^n-\phi_\alpha^n\leq 0 & \forall t\end{array}\right\} \quad \cdots\cdots(3.9)$$

where

$$M_{\alpha\beta}=\int_\Omega N_\alpha\rho N_\beta\,d\Omega \quad \cdots\cdots(3.10)$$

In addition, since $u_\alpha^n=\phi_\alpha^n$ at the contact, we also have impact condition:

$$\left.\begin{array}{l}\dot{u}^n_\alpha=\ddot{u}^n_\alpha=0\\ \quad\text{if } \alpha\text{-th node is in contact}\end{array}\right\} \quad \cdots\cdots(3.11)$$

Release condition also must be considered. Suppose that α-th node is released at time $t+\Delta t$, then we have

$$P^n_\alpha(t+\Delta t)=0\,,\quad \ddot{u}^n_\alpha(t+\Delta t)\neq 0 \quad \cdots\cdots(3.12)$$

At the previous time t, we have the contact condition:

$$P^n_\alpha(t)\neq 0\,,\quad \dot{u}^n_\alpha(t)=0\,,\quad \ddot{u}^n_\alpha(t)=0 \quad \cdots\cdots(3.13)$$

If the Newmark's formula is used for temporal discretization, we have

$$\begin{aligned}\dot{u}^n_\alpha(t+\Delta t)&=\dot{u}^n_\alpha(t)+(1-\gamma)\Delta t\,\ddot{u}^n_\alpha(t)\\&\quad+\gamma\Delta t\,\ddot{u}^n_\alpha(t+\Delta t)\\&=\gamma\Delta t\,\ddot{u}^n_\alpha(t+\Delta t)\end{aligned} \quad \cdots\cdots(3.14)$$

If the Newton's law is held at this node during Δt, it gives

$$\ddot{u}^n_\alpha(t+\Delta t)=P^n_\alpha(t)/m_\alpha \quad \cdots\cdots(3.15)$$

Substitution of (3.15) into (3.14) yields

$$\dot{u}^n_\alpha(t+\Delta t)=\gamma\Delta t P^n_\alpha(t)/m_\alpha \quad \cdots\cdots(3.16)$$

Generally we set $\gamma=1/2$ and if m_α is lumped mass, we have

$$m_\alpha=\rho A\Delta l/2 \quad \cdots\cdots(3.17)$$

where A is a tributary area such that $P^n_\alpha=\sigma^n A$ and Δl is the element length. Substitution of (3.17) into (3.16) yields

$$\dot{u}^n_\alpha(t+\Delta t)=\frac{P^n_\alpha(t)}{\rho A}\frac{\Delta t}{\Delta l} \quad \cdots\cdots(3.18)$$

Equations (3.15) and (3.18) are the release condition for discrete problem. If we choose $\Delta t=\Delta l/C$, i.e. elastic wave travels Δl during Δt, we have

$$\dot{u}^n_\alpha(t+\Delta t)=P^n_\alpha(t)/\rho CA \quad \cdots\cdots(3.19)$$

where C is the velocity of an appropriate elastic wave. This expression is same as the one used by Hughes *et al.*[7].

(2) Temporal Discretization and Solution Algorithm

The matrix equation of motion (3.8) is discretized in time using the Newmark method as follows.

$$\bar{K}u_{t+\Delta t}=\bar{f}_{t+\Delta t} \quad \cdots\cdots(3.20)$$

where effective stiffness matrix:

$$\bar{K}=K+\frac{1}{\beta\Delta t^2}M \quad \cdots\cdots(3.21)$$

effective load vector:

$$\bar{f}_{t+\Delta t}=f_{t+\Delta t}+M\left\{\frac{1}{\beta\Delta t^2}u_t+\frac{1}{\beta\Delta t}\dot{u}_t+\frac{1-2\beta}{2\beta}\ddot{u}_t\right\} \quad \cdots\cdots(3.22)$$

The displacement $\boldsymbol{u}(t+\Delta t)$ must satisfy the boundary condition (3.5), the contact condition (3.7) and the impact condition (3.13), and the release conditions (3.15) and (3.18) when release is noted, for each time step.

Since the effective stiffness matrix $\bar{K}$ is linear and positive definite, we can write, as in section 2.(3),

$$\begin{aligned}u_{t+\Delta t}&=\bar{K}^{-1}\bar{f}_{t+\Delta t}\\&=\hat{u}_{t+\Delta t}+\bar{K}^{-1}P_{t+\Delta t}\end{aligned} \quad \cdots\cdots(3.23)$$

where $\hat{u}_{t+\Delta t}$ is the displacement due to known external load and inertia force, and $\bar{K}^{-1}P_{t+\Delta t}$ is the displacement due to unknown contact pressure $P_{t+\Delta t}$. Since (3.9) is the same form as (2.28), a smooth impact problem can be solved by any one of the algorithms discussed in section 2 for each time step. For an obvious reason (c.f. section 2-(5)), the proposed elimination method is applied here in. The solution algorithm for a smooth impact can be summarized in the following steps:

Step 1: initialization
Step 2: form effective stiffness matrix $\bar{K}$
Step 3: compute $\bar{K}^{-1}$ and form $C_{\alpha\beta}$
Step 4: compute effective load vector $\bar{f}_{t+\Delta t}$
Step 5: solve $\hat{u}_{t+\Delta t}=\bar{K}^{-1}\bar{f}_{t+\Delta t}$
Step 6: compute $\hat{\phi}^n_\alpha=\phi^n_\alpha-\hat{u}^n_\alpha$ and if contact, compute contact force $P_{t+\Delta t}$ as discussed in section 2-(4).
Step 7: $u_{t+\Delta t}=\hat{u}_{t+\Delta t}+\bar{K}^{-1}P_{t+\Delta t}$
Step 8: calculate $\dot{u}_{t+\Delta t}$ and $\ddot{u}_{t+\Delta t}$
if contact, set $\dot{u}_{t+\Delta t}=\ddot{u}_{t+\Delta t}=0$
if release, set

$$\dot{u}_{t+\Delta t}=\frac{P^n_\alpha(t)}{\rho A}\frac{\Delta t}{\Delta l}\,,\quad \ddot{u}_{t+\Delta t}=\frac{P^n_\alpha(t)}{m_\alpha}$$

Continue steps 4~8 till desired time.

(3) Longitudinal Impact of an Elastic Bar

Main objectives here are to see if the contact-impact-release conditions are adequate to describe smooth impacts and to assess computational efficiency of the proposed algorithm when combined with the Newmark time stepping method. The bilinear isoparametric elements are used throughout.

Longitudinal impact of an elastic bar to a smooth rigid wall is first solved. **Fig. 6** shows the finite element mesh and material constants. Newmark data for this problem are (c.f. 16))

Central explicit:	$\beta=0.001001$,	$\gamma=0.502$
Average acceleration:	$\beta=0.25$,	$\gamma=0.5$
Backward:	$\beta=1.0$,	$\gamma=1.5$

and the time step Δt is taken as

$$\Delta t=\frac{\Delta l}{C}=0.01$$

Contact force, displacement, and velocity of free end calculated using lumped mass are shown

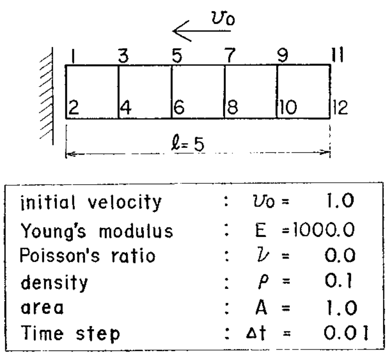

Fig. 6 Finite element mesh for impact of an elastic bar.

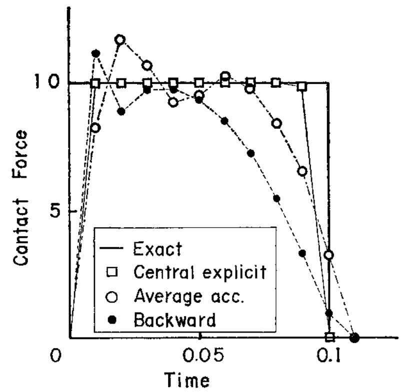

Fig. 7 Impact of an elastic bar, contact force vs. time.

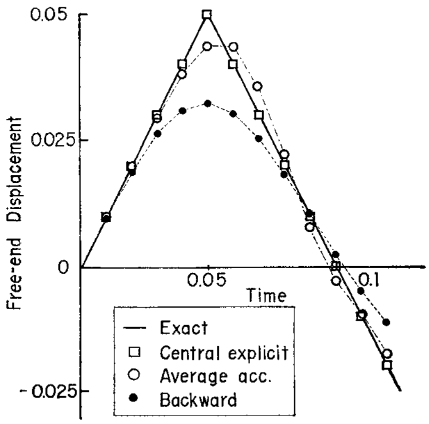

Fig. 8 Impact of an elastic bar, free end displacement vs. time.

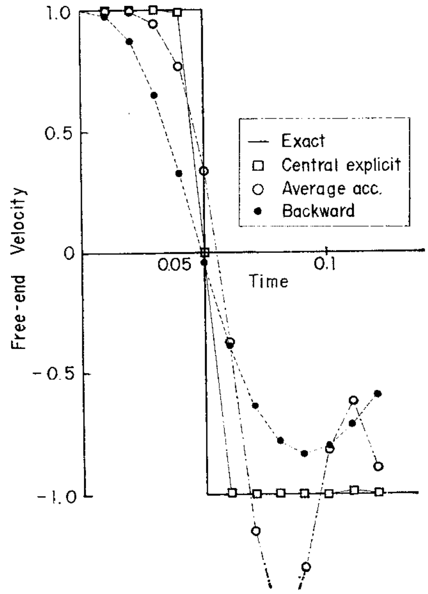

Fig. 9 Impact of an elastic bar, free end velocity vs. time.

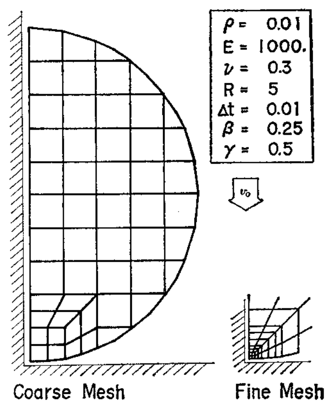

Fig. 10 Finite element mesh for impact of an elastic sphere.

in **Fig. 7~9**. In spite of coarse mesh, the results show good agreement with the exact solution. The accuracy of the central explicit scheme should be noted and it is also found that if the consistent mass is used in the analysis, the central explicit scheme gives unstable solutions while the others give stable results.

(4) Impact of an Elastic Sphere against a Rigid Plane

Fig. 10 shows the finite element mesh and other data used. The coarse mesh consists of 52 elements and 70 nodes, and the fine mesh consists of 72 elements and 95 nodse. **Fig. 11** shows the change of contact force with respect to time. The fine mesh was used. It is observed that numerically obtained maximum contact

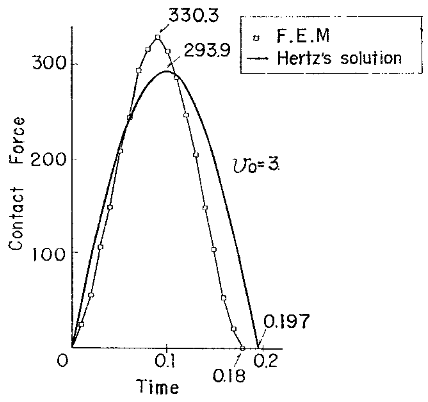

(a) $v_0=3.0$

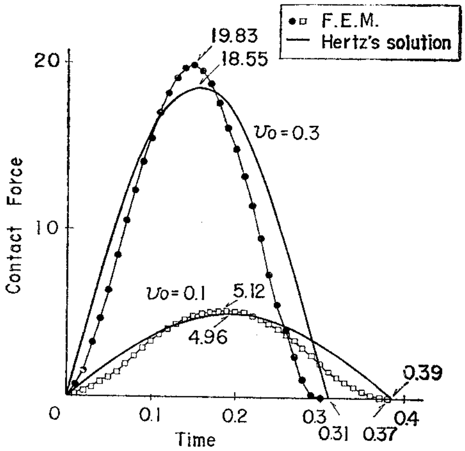

(b) $v_0=0.3$, 0.1

Fig. 11 Impact of an elastic sphere, contact force vs. time.

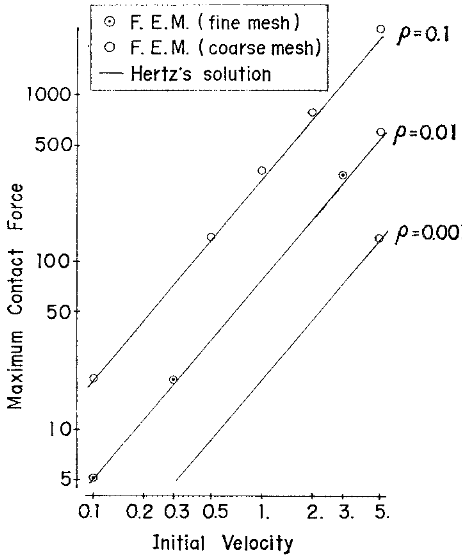

Fig. 12 Impact of an elastic sphere maximum contact force vs. Intial velocity.

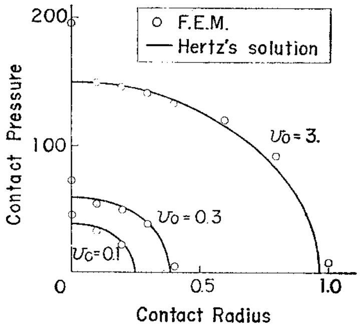

Fig. 13 Impact of an elastic sphere, contact pressure distribution at instant of maximum, contact force.

forces are larger than that of the quasi-static Hertz's solution (c.f. 1)). Calculated duration of impact is shorter than one of the Hertz's solution (**Fig. 11**). Moreover the curve representing contact force and time is different from the sine-curve. These disagreements seem to suggest inadequacy of the quasi-static solution. For further evaluation, the maximum contact forces for various values of density and initial velocity v_0 are plotted in **Fig. 12** which shows effects of density and velocity on contact force despite the possible error due to the coarse mesh used.

Fig. 13 shows the distribution of contact pressure, which is calculated by dividing nodal contact force by tributary area. The numerical result shows a good agreement with the quasi-static Hertz's solution except near the axis of symmetry, where the nodal force consists of delta functions. Contact stress computed by stress on the element boundary gives the better result as opposed to stress computed from the nodal contact force, which agrees with the observation made in 7).

4. CONCLUDING REMARKS

The numerical results of this study show that a smooth contact and impact problem of linear elastic body can be solved successfully using the finite element approximation based on the variational inequalities. The proposed solution algorithm for the resulting system of finite element inequalities works very effectively and this encourages us to solve various static and dynamic problems with inequality constraints, which can be found readily in various engineering fields. However, there remain some difficulties.

A complete mathematical study of the proposed elimination method needs to be done. A very good convergency of elimination method is shown using some numerical examples but these examples are relatively simple and the degree of freedom of a possible contact surface is small. In order to apply the elimination method to more general and complicated problem, its algorithm and convergency must be studied in detail.

Since elimination method is based on the reciprocal formulation, it is necessary to inverse the stiffness matrix explicitly, which will present a problem if the total degree of freedom of the system becomes excessively large. Direct generation of local Green's function and application of boundary elements could be worthwhile to study in the future.

ACKNOWLEDGEMENT: Supports by the Taisei Corp., Ohio State Univ., and NSF (Grant MCS78-04758) are gratefully acknowledged.

REFERENCES

1) Goldsmith, W.: Impact, Edward Arnold, London, 1960.
2) Singorini, A.: Questioni di elastostatica linearizzata e semilinearizzata, Rend. Mat. Appl, XVIII, 1959.
3) Fichera, G.: Problemi elastostatici con vincoli unilaterali il problema die Sigorini con ambigue condizioni al contorno, Mem. Accad. Naz. Lincei, 1964.
4) Lions, J. L. and G. Stampacchia: Variational inequalities, Comm. Pure Appl. Math., XX, 1967.
5) Duvaut, G. and J. L. Lions: Inequalities in Mechanics and Physics, Springer-Verlag, Berlin, 1976.
6) Chan, S. K. and I. S. Tuba: A finite element method for contact problems of solid bodies, Int. J. Mech. Sci., 1971.
7) Hughes, T., R. Taylor, J. Sachman, A. Curnier and W. Kanoknukulchai: A finite element method for a class of contact-impact problems, Comp. Meth. in Appl. Mech. and Engi. 8, 1976.
8) Kalker, J. J. and T. Van Randen: A minimum principle for frictionless elastic contact with application to non-Hertzian half space contact problems, J. Eng. Math, 1972.
9) Conry, T. F. and A. Serireg: A mathematical programming method for design of elastic bodies in contact, J. Appl. Mech., 1971.
10) Kalker, J. J.: Variational principles of contact elastostatics, J. Inst. Math. Appl., 1977.
11) Woodward, W. and B. Paul: Contact stresses for closely conforming bodies—Application to cylinders and spheres, NT 2S, 1976.
12) Panagiotopoulos, P. D.: Analysis of unilateral contact problem, ASCE EM5, 1976.
13) Fremond, M.: Dual formulation for potential and complementary energies, Unilateral boundary conditions. Applications to the finite element method, Math. Finite Ele. Appl. Whiteman Editor, Academic Press, 1973.
14) Kikuchi, N.: A class of Signorini's problems by reciprocal variational inequalities, Proc. Symp. Computational Techniques for Boundary Problem in Appl. Mech., ASME, Dec. 1979.
15) Arrow, K. J. and L. Hurwicz: Studies in linear and non-linear programming, Stanford Univ. Press, 1958.
16) Zienkiewicz, O. C.: The Finite Element Method, 3rd, Ed, McGraw-Hill, 1977.
17) Oden, J. T.: Finite Elements of Nonlinear Continua, McGraw-Hill, 1972.
18) Kikuchi, N. and J. T. Oden: Contact Problem in Elasticity, TICOM Report 79-8, also to be published by SIAM.
19) Luné, A. I.: Three-Dimensional Problems of the Theory of Elasticity, John Wiley & Sons, Inc., 1964.
20) Sneddon, I. M.: The Relation between Load and Penetration in the Axisymmetric Boussinesq Problem for a Punch of Arbitrary Profile, Int. J. Eng. Sci., 1965.
21) Newmark, N. M.: A method for computation of structural dynamics, ASCE, EM3, 1959.

(Recieved March 8, 1980)